Spectroscopic Study of Jet-Cooled Deuterated Porphycenes: Unusual Isotopic Effects on Proton Tunneling

ARTICLE *in* THE JOURNAL OF PHYSICAL CHEMISTRY B · AUGUST 2014

Impact Factor: 3.3 · DOI: 10.1021/jp505553z · Source: PubMed

THE JOURNAL OF PHYSICAL CHEMISTRY B

Article

pubs.acs.org/JPCB

Spectroscopic Study of Jet-Cooled Deuterated Porphycenes: Unusual Isotopic Effects on Proton Tunneling

Ephriem T. Mengesha,[†,‡] Anne Zehnacker-Rentien,[†] J. Sepioł,[‡] M. Kijak,[‡] and J. Waluk*[,‡]

[†]Institut des Sciences Moléculaires d'Orsay, ISMO, CNRS Université Paris Sud, Bât. 210−91405 Orsay Cédex, France

[‡]Institute of Physical Chemistry, Polish Academy of Sciences, Kasprzaka 44/52, 01-224, Warsaw, Poland

Supporting Information

ABSTRACT: Porphycene (Pc) is a well-known model for studying double hydrogen transfer, which shows vibrational-mode-specific tunneling splitting when isolated in supersonic jets or helium nanodroplets. The effect of deuteration on tunneling splitting is reported for jet-cooled heterogeneous, deuterated Pc samples (Pc-d_{mix}) with the prevailing contribution of Pc-d_{12} isotopologue. The sample introduced into the gas phase using laser desorption is studied by means of laser-induced fluorescence (LIF) and single vibronic level fluorescence (SVLF) measurements, in combination with quantum chemical calculations. The influence of molecular symmetry is studied by comparing Pc, Pc-d_{12}, and Pc-d_{11}. The spectra of Pc-d_{12} show strong similarity to those of the parent undeuterated porphycene (Pc). Comparable tunneling splitting is observed in the two isotopologues, both for the 0−0 transition and the most efficient promoting $2A_g$ mode. In contrast, an unusual isotopic effect is observed for the totally symmetrical $4A_g$ mode. While this vibration behaves as a neutral mode in Pc, neither enhancing nor decreasing the tunneling efficiency, it strongly promotes hydrogen transfer in Pc-d_{12}. This observation is explained in terms of modification of the displacement vectors of the $4A_g$ mode upon deuteration. It demonstrates that isotope substitution affects hydrogen transfer even when the weak structural modifications are far from the reaction center, emphasizing the strongly multidimensional nature of the tunneling process.

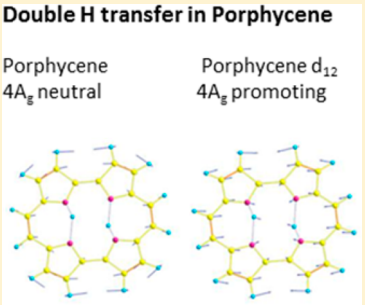

1. INTRODUCTION

Ever since its synthesis[1] as the first known constitutional isomer of porphyrin, porphycene, a tetrapyrrolic macrocycle with four internal nitrogen and two exchangeable hydrogen atoms, continues to be a fascinating molecule for scientists both in fundamental and applied research.[2,3] The structural formulas of porphycene and porphyrin are presented in Scheme 1.

Scheme 1. Porphycene (a) and Porphyrin (b)[a]

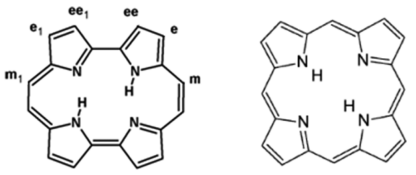

[a]For porphycene, nonequivalent positions of outer rim hydrogens are marked by m for meso hydrogens and e and ee for pyrrole hydrogens.

Although porphycene retains the central feature of porphyrin, it differs in the cavity shape, NH···N distance, and overall symmetry. The structural modification results in the change of symmetry, from D_{2h} in porphyrin to C_{2h} in porphycene. This in turn leads to a change in the intensity pattern of the electronic transitions and overall photophysical properties. For example, porphycene shows much stronger absorption coefficient in a physiologically relevant region (600−650 nm), which makes it a much better agent for photodynamic therapy than porphyrin.[4−10] This behavior is due to a larger |ΔHOMO − ΔLUMO| difference in porphycene than in porphyrin, where ΔHOMO and ΔLUMO are the energy splitting between the HOMO and HOMO−1, and LUMO and LUMO+1, respectively.[11]

In the most stable form of porphycene or porphyrin, the two inner hydrogen atoms are in *trans* position, that is, located at opposite nitrogen atoms, as shown in Scheme 1. Due to the symmetry of the system, the hydrogen atoms can migrate from one *trans* configuration to the other equivalent *trans* tautomer, in a so-called double hydrogen transfer. This tautomerism has been widely studied in porphyrin and porphycene; both molecules are considered as model systems for the double hydrogen transfer reaction.[3,12−40] They strongly differ, however, in the rate and mechanism of tautomerization. The interconversion between the *trans* tautomers of porphyrin is strongly temperature-dependent and has been shown to proceed via a two-step mechanism, involving the *cis* form with the hydrogen atoms located at the neighboring nitrogen atoms as an intermediate.[12−14] In contrast, NMR studies of

Special Issue: Photoinduced Proton Transfer in Chemistry and Biology Symposium

Received: June 5, 2014
Revised: August 18, 2014

   dx.doi.org/10.1021/jp505553z | J. Phys. Chem. B XXXX, XXX, XXX−XXX

crystalline porphycene have shown that the interconversion between the two *trans* forms is very fast on the NMR time scale, even at 107 K.[15]

This observation suggests the tunneling nature of the hydrogen exchange mechanism. Low temperature experiments, performed under supersonic jet[41−43] or helium nanodroplets[44] conditions, are especially informative in this respect and confirm this hypothesis. Sepioł et al.[41] carried out the first supersonic jet study of porphycene which demonstrated that the transition origin and all the vibronic bands observed in the laser-induced fluorescence (LIF) excitation spectrum are split into doublets. The doublets disappear upon exchange of one or both inner protons by deuterons or complexation with water or alcohol. This observation was interpreted as the evidence of coherent double hydrogen tunneling in a symmetric double minimum potential. In general, the observed splittings might depend on the tunneling potentials in both electronic states, but in the present instance, previous work based on the analysis of spectral response to deuteration and to changes in cooling conditions has shown that they are mainly due to the ground state.[41]

The fact that the electronic ground state splitting is much larger than in the S_1 excited state indicates a higher energy barrier or a larger barrier width in the excited state (Figure 1), a

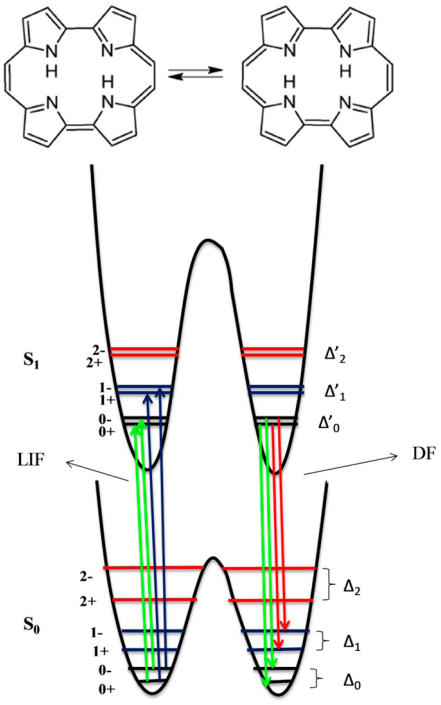

Figure 1. Schematic representation of the ground and excited state potential energy surfaces. The allowed transitions between tunneling levels are indicated by arrows.

situation contrasting with most of the cases observed so far, whether intramolecular, like tropolone,[45−47] or intermolecular, as in benzoic acid dimers.[48,49] This hypothesis was confirmed by polarization spectroscopy measurements in condensed phases, carried out both in emission and transient absorption, which enabled determining the tautomerization rates in S_0 and S_1 for porphycene and several derivatives.[28,35,50,51] The reaction rates in S_1 are several times smaller than in S_0, which can be explained by an increase of the NH···N distance. Moreover, the reaction rates vary by 4 orders of magnitude (10^9−10^{13} s^{-1}) for differently substituted porphycenes. The isotope effects, measured at 293 K, are also substantial.[34,35] These findings indicate the importance of tunneling, even at room temperature, and that of the overall symmetry on the process. In particular, in *meso*-alkylated porphycenes, the alkyl substitution leads to a decrease of the NH···N distance in the cavity, one of the key parameters in proton transfer dynamics. It has been shown also that the torsional modes of the substituents are coupled to the motion of internal protons, resulting in the multidimensional nature of tunneling.[30,32,42]

The vibrational transitions appearing in the dispersed fluorescence spectrum obtained by excitation of the electronic transition origin of porphycene are composed of doublets, differing in the magnitude of the splitting and the intensity distribution.[44] The observed differences reflect different tunneling efficiencies for the respective vibrational modes in the S_0 state. This picture was confirmed by theoretical studies, based on Car−Parrinello molecular dynamics simulations.[27] In a recent work,[43] we carried out LIF excitation near a saturation regime, hole burning spectroscopy, and extensive single vibronic level (SVL) dispersed fluorescence measurements of jet-cooled porphycene, along with quantum chemical calculations. Precise assignments of the bands observed in the S_0 and S_1 states of porphycene have been proposed. On the basis of the values of tunneling splitting for different fundamentals, progressions and combinations of vibronic transitions, we also demonstrated the multidimensional nature of proton tunneling and the importance of mode coupling in influencing the process.

Substitution of the inner protons by deuterons or alkyl substitution of external C−H hydrogens both have dramatic effects on the tunneling rate and/or mechanism, as mentioned above. The effects of the alkyl substitution are 2-fold. Substitution first modifies the electronic distribution within Pc, which in turn alters the NH···N distance. Second, it lowers the overall symmetry of the system and introduces additional frequency modes. To disentangle the electronic from nuclear effects, the effect of weak perturbations brought about by hydrogen/deuterium substitution on the outer rim of porphycene has been studied in detail and is reported here. Full substitution of the outer rim results in Pc-d_{12}, which retains the C_{2h} symmetry of Pc. However, vibrational modifications due to deuteration may lead to a change in the coupling schemes between the reaction coordinates and the other modes. Partial deuteration of the outer rim results in various Pc-d_{11} or Pc-d_{10} species. Most of them undergo small deviations from the symmetrical double minimum character of the potential that governs tautomerization in Pc.

The main purpose of this work is to study the effects of these weak structural changes on double hydrogen tunneling, a phenomenon which can be extremely sensitive even to minor perturbations. We show that the replacement of peripheral protons does not significantly affect the tunneling splitting values observed for the 0−0 transition and for the progression of the promoting $2A_g$ mode. In contrast, the totally symmetrical $4A_g$ mode which is neutral in Pc becomes a promoting mode in Pc-d_{12}. This surprising behavior is explained in terms of modification of the displacement vectors of this mode upon deuteration.

dx.doi.org/10.1021/jp505553z | J. Phys. Chem. B XXXX, XXX, XXX−XXX

2. EXPERIMENTAL AND THEORETICAL METHODS

2.1. Experiment. *Experimental Setup.* In the previously reported work on Pc, the sample was heated to increase its vapor pressure before introduction in the gas phase. This procedure could not be followed here because of fast uncontrolled H/D exchange reactions in the furnace. Pc and its isotopologues were therefore introduced into the gas phase using a homemade laser desorption device.[52,53] The sample was prepared by brushing a few mg of porphycene on a 4 cm long and 0.5 mm wide carbon bar. This technique enabled working with very small sample quantities, about 0.25 mg/h of desorbed matter. A frequency-doubled Nd:YAG laser (532 nm; Continuum Minilite) was used as the desorption source. The beam was propagated by an optical fiber to the surface of the carbon bar with 1.5 to 2 mJ energy per pulse. The sample holder was fixed on a linear translation system, with a translation speed of 1 cm/hour, attached to a pulsed valve (General Valve Parker) with a nozzle diameter of 300 μm. The supersonic expansion was generated by expanding neon at 5 atm as a carrier gas. Fluorescence excitation spectra were obtained by exciting the jet-cooled molecule by a tunable frequency-doubled dye laser (Sirah equipped with Rh6G) pumped by the second harmonic of a Nd:YAG laser (Quanta Ray, Spectra-Physics). The fluorescence signal from the sample was collected perpendicularly to both the exciting light and the molecular beam by a two-lens collecting system and a 25 cm long monochromator (Huet M25) used under broad band conditions, and then detected by a Hamamatsu R2059 photomultiplier tube. Dispersed fluorescence emission spectra were recorded with an intensified and gated CCD camera (Andor Technology) after dispersing the fluorescence through a 60 cm long monochromator with 2400 grooves/mm grating (Jobin Yvon). The resolution of the detection system was typically 3 cm^{-1} (fwhm).

Deuteration of Rim Hydrogens. Perdeuteration of the outer rim hydrogen atoms was achieved by the procedure described in ref 37. Briefly, Pc was heated to 150 °C in 70% D_2SO_4 in D_2O for 24 h and chloroform was added to the cold solution before the latter was neutralized with diluted NaOD/D_2O. Finally, the organic layer was concentrated. The mass spectrum of the deuterated product proved that it contained 31% of Pc-d_{12}, 24% of Pc-d_{11}, 17% of Pc-d_{10}, and 11% of Pc-d_9, while the other isotopologues contributed in negligible amounts. The dominant contribution of Pc-d_{12} over other isotopologues encouraged us to study this heterogeneous sample, called hereafter Pc-d_{mix}.

In Situ Deuteration of Internal Hydrogens. Partial deuteration of the labile cavity NH hydrogens was achieved by fast H/D exchange during the interaction of the desorbed Pc, Pc-d_{11}, or Pc-d_{12} with Ne carrier gas seeded with heavy water (or MeOD). The partial vapor pressure of D_2O in Ne was controlled by a thermostated bath kept at 0 °C. Due to the strong difference in lability between the inner and outer rim hydrogens, the outer rim D/H content of the samples prepared thereby was not modified.

2.2. Calculations. The size of the system precludes the use of correlated methods. Ground state geometry optimizations and frequency calculations were therefore done within the frame of the density functional theory (DFT) at the B3LYP/6-31+G(d,p) level. Time-dependent DFT (TD-DFT) method was used for the excited state calculations with the same functional and basis set using the GAUSSIAN 09 program package.[54] Indeed, this method has been shown to properly describe the $\pi\pi^*$ transition in related porphyrins[55] and has been successfully applied to porphycene.[44]

3. RESULTS AND DISCUSSION

3.1. Theoretical Results. The assignment of the bands observed in the LIF excitation spectrum near the 0−0 transition of Pc-d_{mix} is challenging, due to the possibility of partial deuteration at different positions and the associated slight shifts in absorption. Therefore, except for Pc-d_{12}, it is not an easy task to attribute the bands to specific isotopologues. Predicted hydrogen labilities and calculated shifts will be used to this aim.

The lability of a given site can be qualitatively related to the CH bond length (and hence bond order), which amounts in the ground state to 1.08716/1.08775 Å for m/m1, 1.08169/1.08270 Å for e/e1, and 1.08106/1.08192 Å for ee/ee1. The lowest bond order is thus predicted for the m1 position, which is expected to correspond to the most labile hydrogen. Easier deuteration of meso position in porphyrin has also been reported.[56]

S_0 and S_1 geometry optimizations and frequency calculations have been carried out for (i) Pc and Pc-d_{12}, where all the rim hydrogens are substituted with deuterium, (ii) x-Pc-d_{11}, where all the outer rim hydrogens except at position *x* (*x* = m/m1/e/e1/or ee/ee1, see Scheme 1a) are exchanged by deuteriums, and (iii) Pc-d_8, where all skeletal hydrogens except those at the *meso*-positions (m) are deuterated. The calculated frequencies are listed in Table SI, Supporting Information, together with their experimental counterparts.

The calculated harmonic frequencies have been used to determine the Zero-Point-Energy (ZPE) values in S_0 and S_1, denoted as ZPE(S_0) and ZPE(S_1) in Table 1. The ground state frequencies have been scaled by 0.9640, a scaling factor usually used for this level of calculations.[57] The isotopic shift ΔE_{0-0} of

Table 1. Scaled Zero-Point Energies ZPE (S_0), ZPE (S_1) and 0−0 Electronic Transition Shifts Relative to That of Pc (ΔE_{0-0}) or Pc-d_{12} ($\Delta E_{0\text{-}0}$ vs Pc-d_{12}) of Porphycene Isotopologues Calculated Using TD (DFT)/B3LYP/6-31+G(d,p)[a]

	ZPE (S_0) (kcal/mol)	ZPE (S_1) (kcal/mol)	ΔE_{0-0} (cm^{-1})	ΔE_{0-0} vs Pc-d_{12} (cm^{-1})
Pc				
NHNH	178.60694	176.58445		
NHND	176.58446	174.55725	−1.6	
NDND	174.56191	172.52999	−3.3	
Pc-d_{12}				
NHNH	154.98346	153.05445	32.7	
NHND	152.9604	151.02665	31.0	−1.7
NDND	150.93727	148.99878	29.4	−3.3
Pc-d_8				
	163.02327	161.04944	17.0	−15.7
Pc-d_{11}				
m	156.99176	155.0551	30.0	−2.7
m1	156.99601	155.05248	27.6	−5.1
e	156.93746	155.00175	30.4	−2.3
e1	156.92519	154.98871	30.0	−2.7
ee	156.94061	155.00581	30.7	−2.0
ee1	156.92448	154.99097	31.1	−1.6

[a]The S_0 and S_1 scaling factors amount to 0.9640 and 0.9633, respectively (see text).

dx.doi.org/10.1021/jp505553z | J. Phys. Chem. B XXXX, XXX, XXX−XXX

the electronic transition is the modification of the difference between ZPE(S_0) and ZPE(S_1) by deuteration. For the sake of comparison with the experimental results, Table 1 also gives the isotopic shift relative to Pc-d_{12} (ΔE_{0-0} vs Pc-d_{12}). The experimentally determined position of the 0−0 transition of Pc-d_{12} (section 3.2) was used to find the vibrational scaling factor for the S_1 state in such a way that the calculations reproduce the 32.7 cm^{-1} experimental isotopic shift of Pc-d_{12} relative to parent Pc. Then, the same scaling factor was applied to the other isotopologues. This scaling factor amounts to 0.9633. The detailed calculated shifts are listed in Table SII, together with their experimental counterparts.

The relative isotopic shifts of the various Pc-d_{11} isotopologues depend on the deuteration site. The structures m/m1, e/e1, and ee/ee1 of the Pc-d_{11} species are related to each other by double proton transfer and are therefore tunneling tautomeric pairs. Due to incomplete outer rim deuteration, a slight asymmetry is introduced in Pc-d_{11}. The two members of the tautomeric pair m/m1, e/e1, and ee/ee1 are no longer equivalent as they were in Pc-d_{12}. The consequence of this asymmetry is that each tautomeric pair of Pc-d_{11} has asymmetric zero-point energies in a symmetrical double minimum potential (within Born−Oppenheimer approximation), which is a critical parameter in affecting tunneling splitting. The calculated asymmetry in the ground electronic state is the largest (−5.6 cm^{-1}) for the ee/ee1 pair and the smallest (+1.5 cm^{-1}) for the m/m1 pair. In the excited electronic state, these values differ from those of the ground state and differ from each other. As a result, the two members of a pair have slightly different calculated shifts of the 0−0 transition. We will therefore consider the mean value of the calculated shift; it is the largest (−3.9 cm^{-1}) for deuteration in the m/m1 position, while deuteration at e/e1 or ee/ee1 positions introduces a mean shift of −2.4 or −1.8 cm^{-1} relative to Pc-d_{12}, respectively.

Exchange of the cavity NH hydrogens with deuteriums is predicted to cause a red shift of about −1.6 and −3.3 cm^{-1} for single and double deuteration both in Pc and Pc-d_{12}. Although in the right direction, the calculations underestimate the experimental red shifts of about 24 and 44 cm^{-1} for single and double internal hydrogen/deuterium exchange in Pc, respectively.[41,44]

3.2. S_0−S_1 Excitation Spectrum. LIF excitation spectra of jet-cooled pure Pc and Pc-d_{mix} are presented in Figure 2a and b, respectively. By comparison of the relative intensities of the tunneling doublets of the 0−0 transitions in the LIF spectrum of porphycene, $I(0_+^+)/I(0_-^-)$ = 0.53, and application of Boltzmann distribution for a known energy difference of 4.4 cm^{-1}, we have estimated the vibrational temperature in the supersonic expansion to be 12 K.[58] The detailed procedure is described in the Supporting Information.

The absence of bands due to undeuterated Pc in the spectrum of Pc-d_{mix} is in accordance with mass spectrometry analysis and confirms the efficiency of the deuteration procedure used here. The LIF spectrum of Pc-d_{12} shows close similarity with that of Pc, in particular in the low frequency region. The narrow and intense band at 16210.2 cm^{-1} (band α) is assigned to the 0_+^+ transition origin of Pc-d_{12}, where all peripheral hydrogens of porphycene are substituted by deuteriums. The blue shift of the transition origin of Pc-d_{12} amounts to 32.7 cm^{-1} relative to the transition origin of Pc, indicating that lowering of the zero-point energy due to deuteration is larger in the ground than in the excited electronic

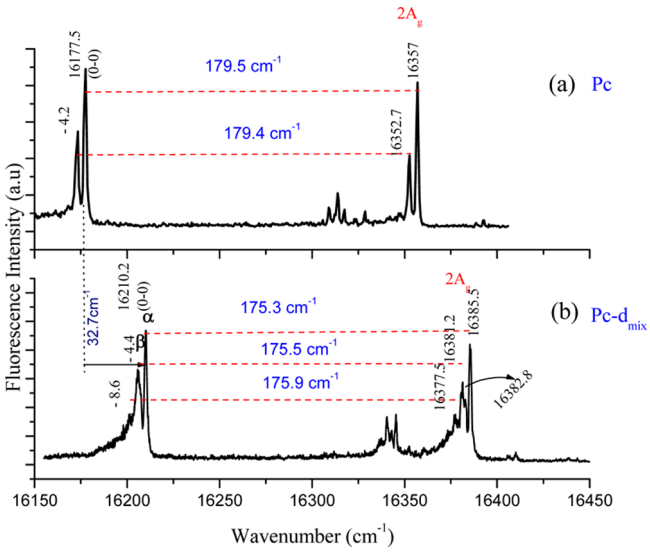

Figure 2. Laser-induced fluorescence excitation spectrum of jet-cooled Pc (a) and Pc-d_{mix} (b).

state. Both blue and red shifts corresponding to a decrease or increase, respectively, of the frequencies upon electronic excitation have been observed in systems showing photo-induced proton transfer.[59−61] Only the modes sensitive to isotopic substitution contribute to the observed effects. Comparison of the calculated frequencies in S_0 and S_1 for Pc and Pc-d_{12} shows that the ν(CH) or ν(NH) stretches as well as the β(NH) bends marginally contribute to the isotopic shift, by less than 1 cm^{-1} for each type of vibration. The role of the in-plane CH bends is more difficult to assess, as these modes are strongly coupled to in-plane CC deformations. It seems, however, that the different contributions cancel out. Last, the out-of-plane CH bends seem to play an important role as they bring an overall contribution to the isotopic shift of more than 20 cm^{-1} to the blue.

A slightly weaker and much broader band (band β) is observed at 16205.8 cm^{-1} (−4.4 cm^{-1} from the 0_+^+ origin of Pc-d_{12}). The band profile is asymmetric due to the expected heterogeneity of the sample. It encompasses the 0_-^- component of the tunneling splitting which will be referred to as the hot band throughout the text. The red shift of the hot band indicates larger tunnelling splitting in the ground state than in the excited state in Pc-d_{12}, as was observed in Pc. The 0_-^- transition is superimposed with significant contributions from various isotopologues with smaller mass, such as Pc-d_{11} and Pc-d_{10}, both eventually showing two tunneling splitting components. The analysis of dispersed fluorescence spectra (section 3.3) measured by excitation at different positions of the asymmetric feature allows assigning the 0−0 transition of Pc-d_{11} and Pc-d_{10} to the bands at 16205.8 (−4.4 cm^{-1} from the 0_+^+ origin of Pc-d_{12}) and 16201.5 cm^{-1} (−8.7 cm^{-1} from the 0_+^+ origin of Pc-d_{12}), respectively. The −4.4 cm^{-1} shift is in good agreement with the calculated mean shift (−3.9 cm^{-1}) caused by the lack of deuterium at the m/m1 positions in the rim of Pc-d_{11}. Moreover, the dominant presence of m/m1/ Pc-d_{11} is in line with the larger lability expected for this structure.

A slightly better resolved feature is observed around 175 cm^{-1} above the origin. By analogy to the band at 179 cm^{-1} in the Pc spectrum, it can be assigned to the $2A_g$ mode. One should notice that the notation $2A_g$ is correct only for Pc and Pc-d_{12}, as both molecules belong to the C_{2h} point groups, but

dx.doi.org/10.1021/jp505553z | J. Phys. Chem. B XXXX, XXX, XXX−XXX

not rigorously correct for the other isotopologues, because they have lower symmetry. However, this notation is adopted for corresponding modes between parent porphycene and its isotopologues. Again, assignment of the contributing isotopologues to their respective spectral features is made possible by a systematic analysis of dispersed fluorescence spectra obtained by selective excitations, as presented in the next section. Anticipating these results, the marked positions at 16385.5, 16381.2, and 16377.5 cm^{-1} (where the latter two bands are located at −4.3 and −8.0 cm^{-1} from the former band, respectively) were assigned to the $2A_g$ mode analogs of Pc-d_{12}, Pc-d_{11}, and Pc-d_{10}, respectively. The shifts and assignments correspond very well to those drawn earlier from the spectral features in the origin region.

It is also informative to check the spectral response of the laser-desorbed sample cooled by Ne carrier gas with D_2O contamination. Due to the lability of the inner hydrogen atoms, they are expected to rapidly exchange with D_2O deuterons, while the outer rim H/D distribution remains unchanged. Figure 3a shows the LIF excitation spectrum of the desorbed

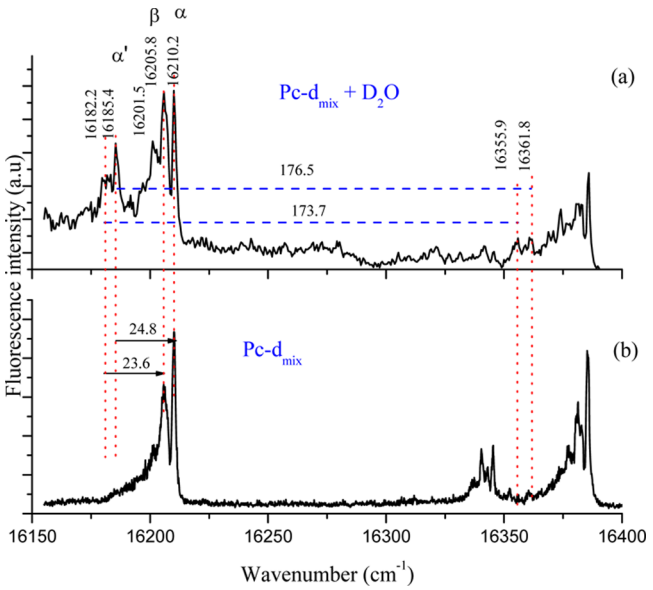

Figure 3. LIF excitation spectrum of jet-cooled Pc-d_{mix} using Ne seeded with D_2O as a carrier gas (a) and pure Ne without D_2O for comparison (b).

sample (Pc-d_{mix}) with heavy water in Ne buffer gas. For comparison, the LIF spectrum of Pc-d_{mix} in pure Ne is shown in Figure 3b.

The optimum signal for spectrum (a) is found at a relatively closer laser-to-nozzle distance than for spectrum (b), which explains a relatively lower signal-to-noise ratio and a higher background in spectrum (a). Comparison of Figure 3a and b shows the appearance of new features in the 16180−16185 range. The most intense band at 16185.4 cm^{-1} (band α') is accompanied by a broad shoulder centered at 16182.2 cm^{-1}. The same pattern is observed in the 16355−16362 cm^{-1} range. Band α' is red-shifted by about 25 cm^{-1} from the 0−0 transition of Pc-d_{12}. A similar red shift (about 24 cm^{-1}) was observed for parent porphycene when one of the internal NH hydrogen was exchanged by deuterium.[41,44] Therefore, we assign band α' to the 0−0 transition of Pc-d_{12+1}, where one of the cavity NH hydrogens in Pc-d_{12} is replaced by deuterium. It is worth noticing that the features observed in the spectrum are characteristic of single deuteration only, in contrast to the effective single and double deuterium exchange observed after conventional heating of porphycene sample in an oven before expansion.[41] This observation can be explained in terms of significantly reduced probability of effective secondary collisions between D_2O and Pc-d_{12+1} due to a limited time in the collision zone in the laser desorption regime, which contrasts to the long interaction between water and Pc when an oven is used.

The weaker intensity shoulder centered at 16182.2 cm^{-1} is assigned to an overlap of 0−0 transitions of various Pc-d_{11+1}, where one of the internal NH hydrogens of Pc-d_{11} is substituted by deuterium. Similar to Pc-d_{12+1}, this band is red-shifted by about 24 cm^{-1} from the 0−0 transition of Pc-d_{11}.

Two other low intensity bands observed at 16355.9 and 16361.8 cm^{-1} (Figure 3a) are shifted by about 175 cm^{-1} relative to the Pc-d_{11+1} and Pc-d_{12+1} origins, respectively. These bands are therefore assigned to the $2A_g$ mode analogues of Pc-d_{11+1} and Pc-d_{12+1} isotopologues, respectively. It is to be noted that the $2A_g$ mode has practically the same frequency whatever the isotopologue, as expected for a mode involving mostly skeletal deformations.

3.3. Single Vibronic Level Fluorescence (SVLF) Spectra. In this section we present SVLF spectra of porphycene isotopologues obtained for the transition origin and higher vibronic levels excitations. Since the $2A_g$ mode is the most prominent tautomerization-promoting mode for which the largest tunnelling splitting of 12 cm^{-1} is found in the ground state of Pc, we exploit this mode as a probe to see subtle effects brought about by deuteration of outer rim hydrogens. Emission resulting from the excitation of other vibronic bands leads to the same conclusion and is presented in the Supporting Information.

3.3.1. Transition Origin (0−0) Excitation. Dispersed fluorescence spectra resulting from the excitation of the 16207.2, 16210.2, 16205.8, and 16201.5 cm^{-1} transitions observed in the LIF excitation spectrum of Pc-d_{mix} are presented in Figure 4a−d, respectively. Based on the excitation spectrum discussed in section 3.2, the three latter features were

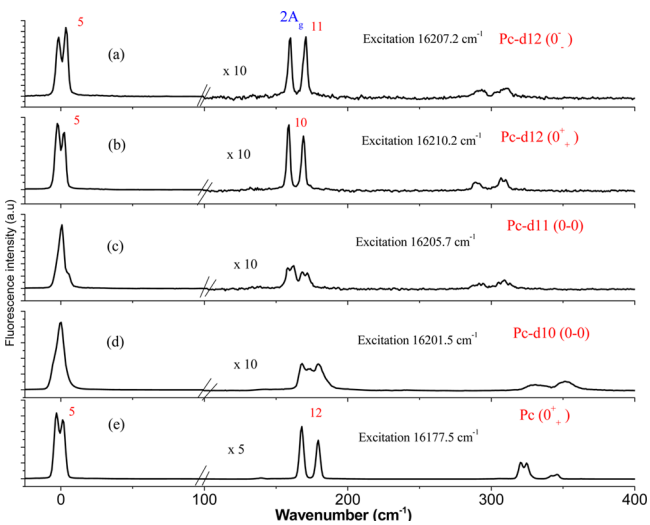

Figure 4. Dispersed fluorescence spectra of jet-cooled porphycene isotopologues. For clarity, the intensities of the spectra in the range 100−400 cm^{-1} are magnified 10× (a−d) or 5× (e).

dx.doi.org/10.1021/jp505553z | J. Phys. Chem. B XXXX, XXX, XXX−XXX

selected as candidates for 0−0 transitions of different isotopologues. As the 16205.8 cm^{-1} band assigned to the 0_-^- transition of Pc-d_{12} overlaps with the origin transition of another isotopologue, emission has been also recorded slightly more to the red, at 16207.2 cm^{-1} where absorption is only due to the 0_-^- transition of Pc-d_{12}. As a reference, Figure 4e shows the dispersed fluorescence spectrum of porphycene resulting from the 0_+^+ excitation.

A glimpse at the spectra recorded for excitation of the bands at 16210.2 and 16207.2 cm^{-1} (Figure 4a,b) shows that they are identical and typical of the excitation of the two components of tunnelling doublets. The spectra also exhibit a pattern similar to that of parent porphycene shown in Figure 4e. The 0−0 transition of Pc-d_{12} is split by practically the same amount as that of parent Pc, despite the fact that the zero-point energy is decreased in the former isotopologue. On the other hand, the $2A_g$ mode appears as a doublet at 158/169 cm^{-1}. Comparison of the tunnelling splitting for the $2A_g$ mode shows only a slight decrease in Pc-d_{12} (10−11 cm^{-1}) compared to parent porphycene (12 cm^{-1}) at the limit of our experimental resolution. Therefore, it is possible to deduce that the low frequency $2A_g$ mode, involving the motion of the internal cavity, does not involve movement of external rim hydrogens. This is confirmed by examining the displacement vectors of the $2A_g$ mode in Pc-d_{12}, which parallel the results of Gawinkowski et al. for Pc.[37] In both Pc and Pc-d_{12}, the C−H stretching modes of the external hydrogens are unaffected by deuteration of the cavity NH hydrogens, showing that the motion of cavity hydrogens is decoupled from the motion of the external hydrogens. This leads to similar behaviors for Pc and Pc-d_{12} in terms of proton tunnelling.

In contrast, the spectra shown in Figure 4c,d are different from each other and from the spectra of Pc or Pc-d_{12}, confirming that they result from the excitation of different species. The 0−0 transitions are broader, indicating the effects of smearing due to the presence of various contributing structures. A closer look at Figure 4c shows that the bands in the range of 170 cm^{-1} appear as doublets of doublets, in contrast to the simple doublets observed in Pc and Pc-d_{12}. This result is in line with our earlier assignment of the band at 16205.8 cm^{-1} in the LIF spectrum (band β) to an overlap of two transitions, namely the 0−0 transition of Pc-d_{11} and the 0_-^- hot band of Pc-d_{12}. Deconvolution of the peaks at about 170 cm^{-1} of the dispersed fluorescence spectrum (see Figure 5) shows four distinct transitions. The pair at 158/168 cm^{-1} belongs to a tunnelling doublet of the $2A_g$ mode of Pc-d_{12}, as mentioned above, while the doublet at 162/171 cm^{-1} belongs to the analogous transitions in Pc-d_{11}.

The large tunnelling splitting depicted in Figure 5 indicates that the $2A_g$ mode acts as a promoting mode for proton tunnelling in Pc-d_{11} as it does in Pc and Pc-d_{12}. The slight decrease of the tunnelling rate in the former can be tentatively explained by the lower symmetry of the molecule (C_s).

Figure 4d presents the dispersed fluorescence (DF) spectrum obtained for excitation of the 16201.5 cm^{-1} peak in the LIF spectrum of Pc-d_{mix}. The resulting DF spectrum bears strong similarity to the other spectra. The congested band at about 175 cm^{-1} is interpreted as the $2A_g$ analogue of various Pc-d_{10} species. The mode which appears as a tunnelling multiplet in Pc, Pc-d_{12} and Pc-d_{11} now appears as a congested feature. The overlap of many bands belonging to several Pc-d_{10} species with various deuteration sites might partially explain the observed spectral congestion.

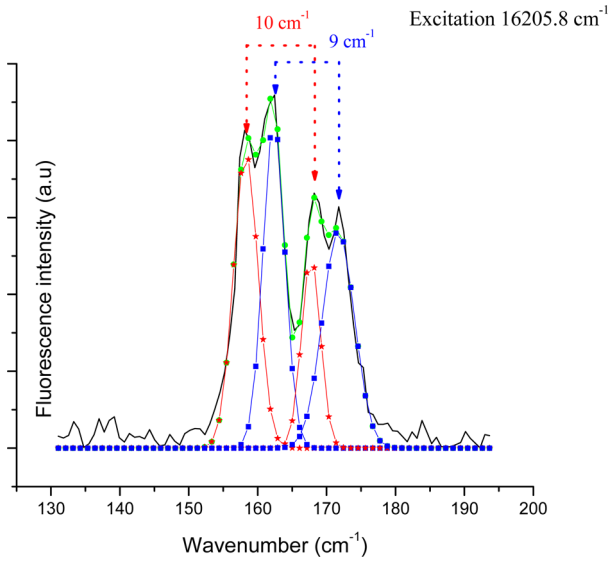

Figure 5. Portions of dispersed fluorescence spectrum of Pc-d_{mix} obtained by excitation at 16205.8 cm^{-1}. Deconvolution of the peaks into bands with Lorentzian line shape shows four distinct transitions. The tunnelling pairs belonging to Pc-d_{12} are indicated by stars, while the tunnelling pairs belonging to Pc-d_{11} species are indicated by squares. The result of the convolution is indicated by circles.

3.3.2. (0−0) + $2A_g$ Excitation. Dispersed fluorescence spectra of porphycene and its isotopologues obtained by excitation of the $2A_g$ mode (0 + 175 cm^{-1}) are presented in Figure 6a−e. The spectra are dominated by the strong $2A_{g1}^1$ transition acting as an origin for a vibrational progression built on the $2A_g$ mode.

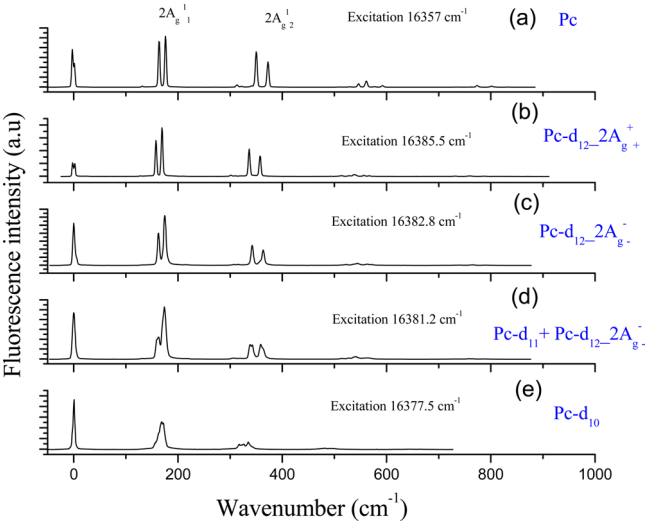

Figure 6. Dispersed fluorescence spectrum of Pc-d_{mix} obtained by excitation of the $2A_{g0}^1$ transition of respective isotopologues.

Figure 6a shows the emission spectrum of the parent porphycene. Two intense doublets are observed at 164/177 cm^{-1} and 351/373 cm^{-1}. They were already assigned[43] to the two tunnelling components of the $2A_{g1}^1$ and $2A_{g2}^1$ transitions, with tunnelling splittings of 13 and 22 cm^{-1}, respectively. The same spectrum for Pc-d_{12} is presented in Figure 6b. As in porphycene, two doublets are observed at 158/170 and 343/364 cm^{-1} with tunnelling splittings of 11 and 21 cm^{-1},

dx.doi.org/10.1021/jp505553z | J. Phys. Chem. B XXXX, XXX, XXX−XXX

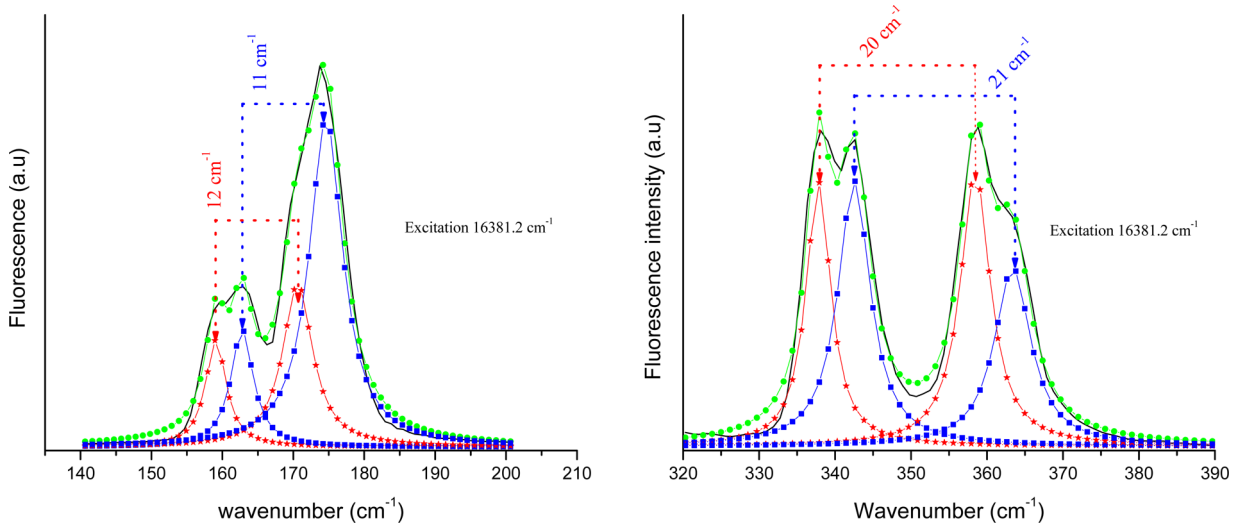

Figure 7. Portions of DF fluorescence spectrum of Pc-d_{mix} obtained by excitation at 16381.2 cm^{-1}. Deconvolution of the peaks into bands with Lorentzian line shape shows four distinct transitions. The tunnelling pairs belonging to Pc-d_{12} are indicated by stars, while the tunnelling pairs belonging to Pc-d_{11} species are indicated by squares. The result of the convolution is indicated by circles.

respectively. These doublets are assigned to the $2A_{g1}^{1}$ and $2A_{g2}^{1}$ transitions of Pc-d_{12}. Apart from a slight difference in the tunnelling splitting value in Pc-d_{12}, as already observed in the dispersed fluorescence spectrum resulting from the excitation of the transition origin, the vibrational pattern is similar to that of parent porphycene. The spectra shown in Figure 6b and c are identical, which is typical of the excitation of the two components of a tunnelling doublet. Therefore, the bands at 16385.5 and 16382.8 cm^{-1} correspond to the $2A_{g0}^{1}0_{+}^{+}$ and $2A_{g}^{1}0_{-}^{-}$ transitions in the LIF spectrum of Pc-d_{12} (Figure 3b). The results also show that tunnelling splitting increases along the vibronic progression built on the $2A_g$ mode both in Pc-d_{12} and Pc-d_{11}, however not linearly, as already reported for Pc.[43] Further, there is no significant difference in tunnelling splitting between the two isotopologues along this mode, as expected for a skeletal deformation mode.

On the other hand, the DF spectrum resulting from the excitation of the 16381.2 cm^{-1} band (Figure 6d) dramatically differs from both Pc and Pc-d_{12}. Around 170 cm^{-1}, doublets of doublets are observed instead of a single doublet, as already described earlier (Figure 4c). A more resolved pattern is observed around 350 cm^{-1}, indicating again a dramatic increase in the tunnelling splitting upon excitation of more quanta of the $2A_g$ mode. Deconvolution of the transitions around 170 and 350 cm^{-1} shows that each of them are composed of four distinct transitions (Figure 7).

It can be deduced from these results that the 16381.2 cm^{-1} band actually is an overlap of two transitions, one corresponding to the $2A_{g0+}^{1+}$ transition of Pc-d_{11} and the other to the hot $2A_{g0-}^{1-}$ transition of Pc-d_{12}. These results are in line with the emission spectra obtained by excitation in the transition origin. The splittings measured here for the $2A_{g0}^{1}$ transition (11 and 12 cm^{-1}) are identical to those of Figure 5, within the error. The splittings amount to 20 and 21 cm^{-1} for the $2A_{g0}^{2}$ transition.

More dramatic spectral change is observed for excitation at 16377.5 cm^{-1} (Figure 6e). A single broad peak appears around 170 cm^{-1}, while a congested band appears around 330 cm^{-1}. The band broadening is explained by the presence of several Pc-d_{10} species formed during the synthesis.

3.3.3. (0−0) + $2A_g$ Excitation: Response to NH/ND Exchange in the Internal Cavity. The direct proof of hydrogen tunnelling in porphycene was provided by the dramatic decrease of the splitting of vibronic transitions upon internal NH/ND exchange.[41,44] Expecting similar effects, we have recorded the dispersed fluorescence spectra obtained via $2A_{g0}^{1}$ excitation of Pc-d_{12}/Pc-d_{12+1}, and Pc-d_{11} /Pc-d_{11+1}, respectively (Figure 8a−d).

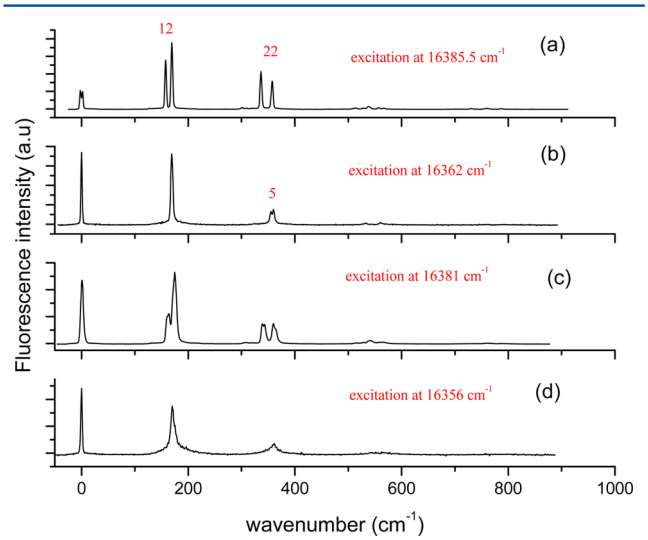

Figure 8. Dispersed fluorescence spectrum of Pc-d_{12} (a), Pc-d_{12+1} (b), Pc-d_{11} (c), and Pc-d_{11+1} (d) via excitation of the $2A_g$ mode.

Comparison of Figure 8a and b shows that the splitting of the $2A_{g1}^{1}$ transition vanishes upon deuteration of one of the exchangeable NH hydrogens in Pc-d_{12}, whereas for the $2A_{g2}^{1}$ transition the value of tunnelling splitting decreases from about 20 cm^{-1} in Pc-d_{12} to 5 cm^{-1} in Pc-d_{12+1}. On the other hand, comparison of Figure 8c and d shows that the doublets in Pc-d_{11} are collapsed into a single broad band as a result of deuteration of one of the internal hydrogens in Pc-d_{11+1}. These experimental results clearly confirm that the origin of the doublet originates from tunnelling both in Pc-d_{12} and Pc-d_{11}

dx.doi.org/10.1021/jp505553z | J. Phys. Chem. B XXXX, XXX, XXX−XXX

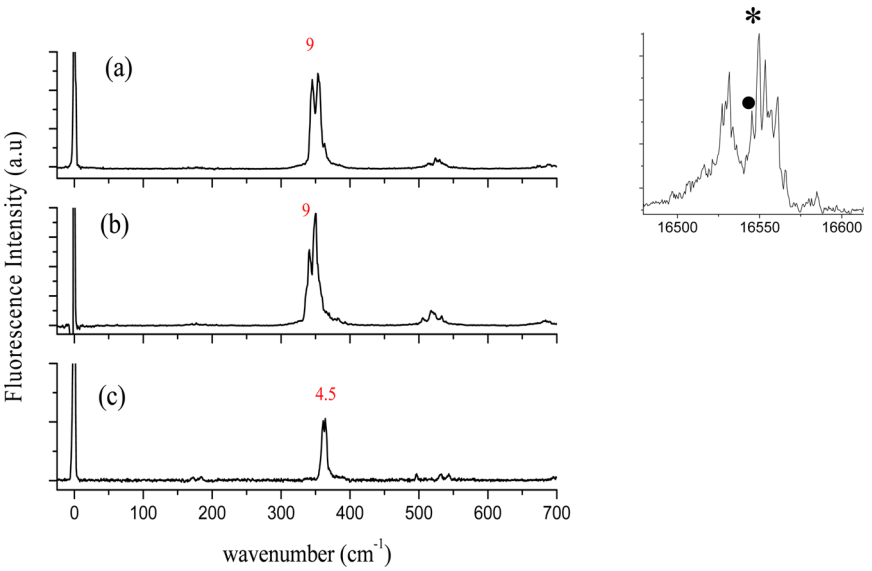

Figure 9. Dispersed fluorescence spectrum of (a) Pc-d_{12}, $4A_{g0}^{1}$ 0_{+}^{+} excitation at 16550 cm^{-1} (asterisk); (b) Pc-d_{12}, $4A_{g0-}^{1-}$ excitation at 16545.4 cm^{-1} (dot); (c) Pc, $4A_{g0+}^{1+}$ excitation. The inset shows part of the LIF spectrum of Pc-d_{mix} and the asterisk and the dot show the position of the tunnelling doublet of the 4Ag mode of Pc-d_{12}.

isotopologues, as it did in Pc, and that deuteration of the inner cavity quenches the tunnelling process.

3.3.4. (0−0) + $4A_g$ Excitation: Reversed Isotopic Effect. Figure 9a,b presents the emission spectra of Pc-d_{mix} obtained by excitation in the $4A_{g0}^{1}$ region. The spectrum resulting from the $4A_{g0}^{1}$ excitation of Pc is shown for comparison in Figure 9c. The three spectra are similar and dominated by the ν_1^1 transition acting as a progression origin. Figure 9a shows the emission spectrum resulting from the excitation of the strong band at 16550 cm^{-1} in the LIF spectrum, located at 339.6 cm^{-1} above the 0−0 transition of Pc-d_{12}. It is dominated by a doublet at 345/354 cm^{-1}. It is easily assigned to the $4A_g$ mode, split by hydrogen tunnelling, on the basis of comparison with Pc and with calculated harmonic frequencies which amount to 348 and 352 cm^{-1} in the S_1 and S_0 states, respectively. Similarly, Figure 9b shows the dispersed fluorescence spectrum obtained by excitation of the band at 16545.4 cm^{-1}, located at 335 cm^{-1} above the 0−0 transition of Pc-d_{12}. The spectra shown in Figure 9a,b are similar, indicating excitation of tunnelling components of the same mode. Thus, the bands at 16545.4 and 16550 cm^{-1} are the $2A_{g0+}^{1+}$ and $2A_{g0-}^{1-}$ transitions of Pc-d_{12}, while the bands at 345/354 cm^{-1} in the emission spectrum are their counterparts in the ground state.

An interesting isotopic effect is observed when comparing the ground state tunnelling splitting of the $4A_g$ mode in Pc and Pc-d_{12}. This mode was identified as neutral, neither promoting proton tunnelling nor inhibiting it in porphycene,[43,44] with tunnelling splitting of 4.5 cm^{-1} similar to that of the vibrationless level of the ground state. Surprisingly, however, the tunnelling splitting of this mode in Pc-d_{12} is found to be twice as large as in Pc in the ground state.

The increase in tunnelling splitting in Pc-d_{12}, at first surprising and contrary to the expectation, can be explained by the analysis of the displacement vectors of the $4A_g$ mode in the ground state, shown in Figures 10a and b for Pc and Pc-d_{12}, respectively.

Only the outer rim hydrogens and carbons show sizable displacement in Pc, while in Pc-d_{12} there is also a significant displacement of the cavity nitrogens and the inner hydrogens in addition to the external hydrogens. This results in modification of the NH···N distance in Pc-d_{12}, but not in Pc, upon excitation of the $4A_g$ mode. Therefore, the increase in tunnelling splitting of the $4A_g$ mode in Pc-d_{12} can be ascribed to modification of the NH···N distance. This finding shows that deuteration affects not only the frequency of vibrations, but also the nature of displacement vectors of some modes, as already calculated for free base porphyrin.[62] Such an effect was also observed in deuterated tropolones (TRN), where the tunnelling splitting in mode ν_{13} of 5D-TRN is larger than the corresponding mode in the parent TRN.[47]

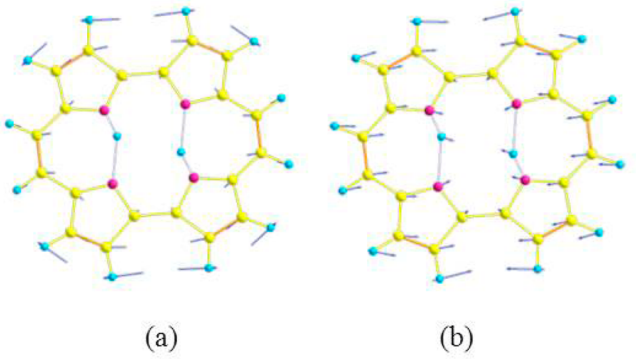

Figure 10. Displacement vectors of the $4A_g$ normal mode of Pc (a) and Pc-d_{12} (b) obtained at the B3LYP/6-31+G(d,p) level.

4. SUMMARY AND CONCLUSIONS

LIF and SVLF measurements, in combination with quantum chemical calculations were applied to investigate heterogeneous, deuterated Pc samples (Pc-d_{mix}) with prevailing contribution of Pc-d_{12}. Comparison of Pc-d_{12} with parent, undeuterated porphycene reveals similar spectroscopic features in the two isotopologues. Comparable tunneling splittings are observed both for 0−0 transition and for the most efficient promoting mode, namely, $2A_g$. Slightly smaller values of tunneling splitting are observed for $2A_g$ in Pc-d_{12}; however, the

dx.doi.org/10.1021/jp505553z | J. Phys. Chem. B XXXX, XXX, XXX−XXX

decrease of 1−2 cm^{-1} is close to the spectral resolution of our equipment.

One could thus conclude from these results that the CH−involving vibrations do not effectively couple to the hydrogen transfer motion. However, deuteration can lead to a change in the form of other normal modes, as demonstrated by the interesting isotopic effect observed via comparison of $4A_g$ modes of Pc and Pc-d_{12}. The $4A_g$ mode is known to be neutral in Pc, that is, exhibiting practically the same value of the splitting as the 0−0 transition. However, in Pc-d_{12}, this mode shows twice the value of the tunneling splitting of the transition origin. This observation was explained in terms of the modification of the displacement vectors of the $4A_g$ mode upon deuteration, which, in turn, increases the coupling to the reaction coordinate. The $4A_g$ mode, neutral in undeuterated Pc, becomes a promoting mode in Pc-d_{12}. This finding opens new perspectives for the studies of other porphycene isotopologues, for example, those with ^{15}N. It could also motivate theoretical calculations of the mode-specificity of the tunneling splitting similar to those recently performed for Pc and Pc-d_1.[63]

Comparison of the spectra of Pc with those of *x*-Pc-d_{11} and Pc-d_{10} species revealed similarities as well as differences. Broadening instead of splitting in the 0−0 transitions of the latter two species, both in the LIF and DF spectra, probably results from large heterogeneity of the sample. On the other hand, similar tunneling splittings are found for Pc, Pc-d_{12}, and *x*-Pc-d_{11} along the most promoting $2A_g$ mode.

Successful measurement of the LIF and DF spectra of Pc and its isotopologues isolated in supersonic jet using laser desorption shows that this technique is promising for the study of proton tunneling in derivatives of porphycene which were previously inaccessible with conventional heating techniques, either due to high melting points of the derivatives or to uncontrolled H/D exchange reactions in the furnace. Our results demonstrate the potential of supersonic jet spectroscopy for the analysis of heterogeneous samples, consisting of isotopologues which are extremely difficult to separate by other methods.

■ ASSOCIATED CONTENT

Supporting Information

Details of the assignment of the two components of the tunneling doublet are given, as well as the analysis of the emission spectra resulting from the excitation of the bands located at (0−0) + 126, 131 and 136, 317, 321, 335, 340, 343, 346, 351, and 356 cm^{-1}. This material is available free of charge via the Internet at http://pubs.acs.org.

■ AUTHOR INFORMATION

Corresponding Author

*E-mail: jwaluk@ichf.edu.pl.

Notes

The authors declare no competing financial interest.

■ ACKNOWLEDGMENTS

This work was supported by the National Science Centre Grant (DEC-2011/02/A/ST5/00443) and by PL-Grid Infrastructure. J.S. and E.M. acknowledge the International Ph.D. Projects Program cofinanced by the Foundation for Polish Science and the European Regional Development Fund within the Innovative Economy Operational Program, "Grants for Innovation". We acknowledge the use of the computing facility cluster GMPCS of the LUMAT federation (FR LUMAT 2764). We are grateful to Dr. Sylwester Gawinkowski for his help in the synthesis of deuterated porphycene.

■ REFERENCES

(1) Vogel, E.; Kocher, M.; Schmickler, H.; Lex, J. Porphycene - a Novel Porphin Isomer. *Angew. Chem., Int. Ed.* **1986**, *25*, 257−259.

(2) Sanchez-Garcia, D.; Sessler, J. L. Porphycenes: Synthesis and Derivatives. *Chem. Soc. Rev.* **2008**, *37*, 215−232.

(3) Waluk, J. Structure, Spectroscopy, Photophysics, and Tautomerism of Free-Base Porphycenes and Other Porphyrin Isomers. In *Handbook of Porphyrin Science*; Smith, K., Kadish, K., Guilard, R., Ed.; World Scientific: Singapore, 2010; Vol. 7, p 359.

(4) Braslavsky, S. E.; Muller, M.; Martire, D. O.; Porting, S.; Bertolotti, S. G.; Chakravorti, S.; KocWeier, G.; Knipp, B.; Schaffner, K. Photophysical Properties of Porphycene Derivatives (18 Pi Porphyrinoids). *J. Photochem. Photobiol. B* **1997**, *40*, 191−198.

(5) Stockert, J. C.; Cañete, M.; Juarranz, A.; Villanueva, A.; Horobin, R. W.; Borrell, J.; Teixidó, J.; Nonell, S. Porphycenes: Facts and Prospects in Photodynamic Therapy of Cancer. *Curr. Med. Chem.* **2007**, *14*, 997−1026.

(6) Richert, C.; Wessels, J. M.; Müller, M.; Kisters, M.; Benninghaus, T.; Goetz, A. E. Photodynamic Antitumor Agents: *β*-Methoxyethyl Groups Give Access to Functionalized Porphycenes and Enhance Cellular Uptake and Activity. *J. Med. Chem.* **1994**, *37*, 2797−2807.

(7) Nonell, S.; Bou, N.; Borrell, J. I.; Teixido, J.; Villanueva, A.; Juarranz, A.; Canete, M. Synthesis of 2,7,12,17-Tetraphenylporphycene (Tppo) - First Aryl-Substituted Porphycene for the Photodynamic Therapy of Tumors. *Tetrahedron Lett.* **1995**, *36*, 3405−3408.

(8) Milanesi, C.; Biolo, R.; Jori, G.; Schaffner, K. Experimental Photodynamic Therapy with Tetrapropyl-Porphycene: Ultrastructural Studies on the Mechanism of Tumour Photodamage. *Lasers Med. Sci.* **1991**, *6*, 437−442.

(9) Mak, N. K.; Kok, T. W.; Wong, R. N. S.; Lam, S. W.; Lau, Y. K.; Leung, W. N.; Cheung, N. H.; Huang, D. P.; Yeung, L. L.; Chang, C. K. Photodynamic Activities of Sulfonamide Derivatives of Porphycene on Nasopharyngeal Carcinoma Cells. *J. Biomed. Sci.* **2003**, *10*, 418−429.

(10) Baumer, D.; Maier, M.; Engl, R.; Szeimies, R. M.; Baumler, W. Singlet Oxygen Generation by 9-Acetoxy-2,7,12,17-Tetrakis(*β*-Methoxyethyl)-Porphycene (ATMPN) in Solution. *Chem. Phys.* **2002**, *285*, 309−318.

(11) Waluk, J.; Müller, M.; Swiderek, P.; Köcher, M.; Vogel, E.; Hohlneicher, G.; Michl, J. Electronic States of Porphycenes. *J. Am. Chem. Soc.* **1991**, *113*, 5511−5527.

(12) Schlabach, M.; Wehrle, B.; Rumpel, H.; Braun, J.; Scherer, G.; Limbach, H. H. NMR and NIR Studies of the Tautomerism of 5,10,15,20-Tetraphenylporphyrin Including Kinetic HH/HD/DD Isotope and Solid-State Effects. *Ber. Bunsen-Ges.* **1992**, *96*, 821−833.

(13) Braun, J.; Schlabach, M.; Wehrle, B.; Kocher, M.; Vogel, E.; Limbach, H. H. Nmr-Study of the Tautomerism of Porphyrin Including the Kinetic HH/HD/DD Isotope Effects in the Liquid and the Solid-State. *J. Am. Chem. Soc.* **1994**, *116*, 6593−6604.

(14) Braun, J.; Limbach, H. H.; Williams, P. G.; Morimoto, H.; Wemmer, D. E. Observation of Kinetic Tritium Isotope Effects by Dynamic NMR. The Tautomerism of Porphyrin. *J. Am. Chem. Soc.* **1996**, *118*, 7231−7232.

(15) Wehrle, B.; Limbach, H. H.; Kocher, M.; Ermer, O.; Vogel, E. N-15-CPMAS-NMR Study of the Problem of NH Tautomerism in Crystalline Porphine and Porphycene. *Angew. Chem., Int. Ed.* **1987**, *26*, 934−936.

(16) Langer, U.; Hoelger, C.; Wehrle, B.; Latanowicz, L.; Vogel, E.; Limbach, H. H. N-15 NMR Study of Proton Localization and Proton Transfer Thermodynamics and Kinetics in Polycrystalline Porphycene. *J. Phys. Org. Chem.* **2000**, *13*, 23−34.

(17) Pietrzak, M.; Shibl, M. F.; Bröring, M.; Kühn, O.; Limbach, H. H. $^1H/^2H$ NMR Studies of Geometric H/D Isotope Effects on the

Coupled Hydrogen Bonds in Porphycene Derivatives. *J. Am. Chem. Soc.* **2007**, *129*, 296−304.
(18) Shibl, M. F.; Pietrzak, M.; Limbach, H. H.; Kuhn, O. Geometric H/D Isotope Effects and Cooperativity of the Hydrogen Bonds in Porphycene. *ChemPhysChem* **2007**, *8*, 315−321.
(19) del Amo, J. M. L.; Langer, U.; Torres, V.; Pietrzak, M.; Buntkowsky, G.; Vieth, H. M.; Shibl, M. F.; Kuhn, O.; Broring, M.; Limbach, H. H. Isotope and Phase Effects on the Proton Tautomerism in Polycrystalline Porphycene Revealed by Nmr. *J. Phys. Chem. A* **2009**, *113*, 2193−2206.
(20) Kozlowski, P. M.; Zgierski, M. Z.; Baker, J. The Inner-Hydrogen Migration and Ground-State Structure of Porphycene. *J. Chem. Phys.* **1998**, *109*, 5905−5913.
(21) Smedarchina, Z.; Shibl, M. F.; Kuhn, O.; Fernandez-Ramos, A. The Tautomerization Dynamics of Porphycene and Its Isotopomers - Concerted Versus Stepwise Mechanisms. *Chem. Phys. Lett.* **2007**, *436*, 314−321.
(22) Smedarchina, Z.; Siebrand, W.; Fernandez-Ramos, A.; Meana-Paneda, R. Mechanisms of Double Proton Transfer. Theory and Applications. *Z. Phys. Chem.* **2008**, *222*, 1291−1309.
(23) Duran-Frigola, M.; Tejedor-Estrada, R.; Sanchez-Garcia, D.; Nonell, S. Dual Fluorescence in 9-Amino-2,7,12,17-Tetraphenylporphycene. *Phys. Chem. Chem. Phys.* **2011**, *13*, 10326−10332.
(24) Waluk, J. Ground- and Excited-State Tautomerism in Porphycenes. *Acc. Chem. Res.* **2006**, *39*, 945−952.
(25) Waluk, J. Tautomerization in Porphycenes. In *Hydrogen-Transfer Reactions*; Hynes, J. T., Klinman, J. P., Limbach, H. H., Schowen, R. L., Eds. Wiley-VCH: Weinheim, 2007; Vol. *1*, pp 245−271.
(26) Waluk, J. Porphycenes: Spectroscopy, Photophysics, and Tautomerism. In *CRC Handbook of Organic Photochemistry and Photobiology*; Oelgemoeller, M., Griesbeck, A., Ghetti, F., Eds.; Taylor and Francis: U.K., 2011.
(27) Walewski, L.; Waluk, J.; Lesyng, B. Car-Parrinello Molecular Dynamics Study of the Intramolecular Vibrational Mode-Sensitive Double Proton-Transfer Mechanisms in Porphycene. *J. Phys. Chem. A* **2010**, *114*, 2313−2318.
(28) Gil, M.; Waluk, J. Vibrational Gating of Double Hydrogen Tunneling in Porphycene. *J. Am. Chem. Soc.* **2007**, *129*, 1335−1341.
(29) Piwonski, H.; Hartschuh, A.; Urbanska, N.; Pietraszkiewicz, M.; Sepiol, J.; Meixner, A. J.; Waluk, J. Polarized Spectroscopy Studies of Single Molecules of Porphycenes: Tautomerism and Orientation. *J. Phys. Chem. C* **2009**, *113*, 11514−11519.
(30) Piwonski, H.; Sokolowski, A.; Kijak, M.; Nonell, S.; Waluk, J. Arresting Tautomerization in a Single Molecule by the Surrounding Polymer: 2,7,12,17-Tetraphenyl Porphycene. *J. Phys. Chem. Lett.* **2013**, *4*, 3967−3971.
(31) Piwoński, H.; Stupperich, C.; Hartschuh, A.; Sepioł, J.; Meixner, A.; Waluk, J. Imaging of Tautomerism in a Single Molecule. *J. Am. Chem. Soc.* **2005**, *127*, 5302−5303.
(32) Gil, M.; Dobkowski, J.; Wiosna-Salyga, G.; Urbanska, N.; Fita, P.; Radzewicz, C.; Pietraszkiewicz, M.; Borowicz, P.; Marks, D.; Glasbeek, M.; Waluk, J. Unusual, Solvent Viscosity-Controlled Tautomerism and Photophysics: Meso-Alkylated Porphycenes. *J. Am. Chem. Soc.* **2010**, *132*, 13472−13485.
(33) Gil, M.; Organero, J. A.; Waluk, J.; Douhal, A. Ultrafast Dynamics of Alkyl-Substituted Porphycenes in Solution. *Chem. Phys. Lett.* **2006**, *422*, 142−146.
(34) Fita, P.; Urbanska, N.; Radzewicz, C.; Waluk, J. Unusually Slow Intermolecular Proton-Deuteron Exchange in Porphycene. *Z. Phys. Chem.* **2008**, *222*, 1165−1173.
(35) Fita, P.; Urbanska, N.; Radzewicz, C.; Waluk, J. Ground- and Excited-State Tautomerization Rates in Porphycenes. *Chem.—Eur. J.* **2009**, *15*, 4851−4856.
(36) Gawinkowski, S.; Orzanowska, G.; Izdebska, K.; Senge, M. O.; Waluk, J. Bridging the Gap between Porphyrins and Porphycenes: Substituent-Position-Sensitive Tautomerism and Photophysics in Meso-Diphenyloctaethylporphyrins. *Chem.—Eur. J.* **2011**, *17*, 10039−10049.
(37) Gawinkowski, S.; Walewski, L.; Vdovin, A.; Slenczka, A.; Rols, S.; Johnson, M. R.; Lesyng, B.; Waluk, J. Vibrations and Hydrogen Bonding in Porphycene. *Phys. Chem. Chem. Phys.* **2012**, *14*, 5489−5503.
(38) Sobolewski, A. L.; Gil, M.; Dobkowski, J.; Waluk, J. On the Origin of Radiationless Transitions in Porphycenes. *J. Phys. Chem. A* **2009**, *113*, 7714−7716.
(39) Kumagai, T.; Hanke, F.; Gawinkowski, S.; Sharp, J.; Kotsis, K.; Waluk, J.; Persson, M.; Grill, L. Thermally and Vibrationally Induced Tautomerization of Single Porphycene Molecules on a Cu(110) Surface. *Phys. Rev. Lett.* **2013**, *111*.
(40) Kumagai, T.; Hanke, F.; Gawinkowski, S.; Sharp, J.; Kotsis, K.; Waluk, J.; Persson, M.; Grill, L. Controlling Intramolecular Hydrogen Transfer in a Porphycene Molecule with Single Atoms or Molecules Located Nearby. *Nat. Chem.* **2014**, *6*, 41−46.
(41) Sepioł, J.; Stepanenko, Y.; Vdovin, A.; Mordziński, A.; Vogel, E.; Waluk, J. Proton Tunnelling in Porphycene Seeded in a Supersonic Jet. *Chem. Phys. Lett.* **1998**, *296*, 549−556.
(42) Vdovin, A.; Sepiol, J.; Urbanska, N.; Pietraszkiewicz, M.; Mordzinski, A.; Waluk, J. Evidence for Two Forms, Double Hydrogen Tunneling, and Proximity of Excited States in Bridge-Substituted Porphycenes: Supersonic Jet Studies. *J. Am. Chem. Soc.* **2006**, *128*, 2577−2586.
(43) Mengesha, E. T.; Sepiol, J.; Borowicz, P.; Waluk, J. Vibrations of Porphycene in the S-0 and S-1 Electronic States: Single Vibronic Level Dispersed Fluorescence Study in a Supersonic Jet. *J. Chem. Phys.* **2013**, *138*, 174201.
(44) Vdovin, A.; Waluk, J.; Dick, B.; Slenczka, A. Mode-Selective Promotion and Isotope Effects of Concerted Double-Hydrogen Tunneling in Porphycene Embedded in Superfluid Helium Nanodroplets. *ChemPhysChem* **2009**, *10*, 761−765.
(45) Ensminger, F. A.; Plassard, J.; Zwier, T. S.; Hardinger, S. Mode-Selective Photoisomerization in 5-Hydroxytropolone. I. Experiment. *J. Chem. Phys.* **1995**, *102*, 5246−5259.
(46) Nash, J. J.; Zwier, T. S.; Jordan, K. D. Mode-Selective Photoisomerization in 5-Hydroxytropolone. II. Theory. *J. Chem. Phys.* **1995**, *102*, 5260−5270.
(47) Sekiya, H.; Nagashima, Y.; Tsuji, T.; Nishimura, Y.; Mori, A.; Takeshita, H. Vibrational Mode-Specific Tunneling Splittings in the Approximately-a States of Deuterated Tropolones. *J. Phys. Chem.* **1991**, *95*, 10311−10317.
(48) Florio, G. M.; Sibert, E. L.; Zwier, T. S. Fluorescence-Dip IR Spectra of Jet-Cooled Benzoic Acid Dimer in Its Ground and First Excited Singlet States. *Faraday Discuss.* **2001**, *118*, 315−330.
(49) Florio, G. M.; Zwier, T. S.; Myshakin, E. M.; Jordan, K. D.; Sibert, E. L. Theoretical Modeling of the Oh Stretch Infrared Spectrum of Carboxylic Acid Dimers Based on First-Principles Anharmonic Couplings. *J. Chem. Phys.* **2003**, *118*, 1735−1746.
(50) Fita, P.; Ciacka, P.; Czerski, I.; Pietraszkiewicz, M.; Radzewicz, C.; Waluk, J. Double Hydrogen Transfer in Low Symmetry Porphycenes. *Z. Phys. Chem.* **2013**, *227*, 1009−1020.
(51) Fita, P.; Garbacz, P.; Nejbauer, M.; Radzewicz, C.; Waluk, J. Ground and Excited State Double Hydrogen Transfer in Symmetric and Asymmetric Potentials: Comparison of 2,7,12,17-Tetra-*N*-propylporphycene with 9-Acetoxy-2,7,12,17-tetra-*N*-propylporphycene. *Chem.—Eur. J.* **2011**, *17*, 3672−3678.
(52) Piuzzi, F.; Dimicoli, I.; Mons, M.; Tardivel, B.; Zhao, Q. C. A Simple Laser Vaporization Source for Thermally Fragile Molecules Coupled to a Supersonic Expansion: Application to the Spectroscopy of Tryptophan. *Chem. Phys. Lett.* **2000**, *320*, 282−288.
(53) Sen, A.; Bouchet, A.; Lepere, V.; Le Barbu-Debus, K.; Scuderi, D.; Piuzzi, F.; Zehnacker-Rentien, A. Conformational Analysis of Quinine and Its Pseudo Enantiomer Quinidine: A Combined Jet-Cooled Spectroscopy and Vibrational Circular Dichroism Study. *J. Phys. Chem. A* **2012**, *116*, 8334−8344.
(54) Frisch, M.; et al. *Gaussian 09*, Revision B.01; Gaussian, Inc.: Wallingford, CT, 2010.
(55) Baerends, E. J.; Ricciardi, G.; Rosa, A.; van Gisbergen, S. J. A. A DFT/TDDFT Interpretation of the Ground and Excited States of

Porphyrin and Porphyrazine Complexes. *Coord. Chem. Rev.* **2002**, *230*, 5−27.
(56) Ksenofontova, N. K.; Gradyushko, A. T.; Solov'ev, K. N.; Starkhin, A. S.; Shul'ga, A. M. Resonance Raman Spetra of Porphyn and Its Deuterium Derivatives. *Zh. Prikl. Spektrosk.* **1976**, *25*, 841−849.
(57) http://cccbdb.nist.gov/vibscalejust.asp.
(58) Sepiol, J.; Stepanenko, Y.; Vdovin, A.; Mordzinski, A.; Vogel, E.; Waluk, J. Proton Tunnelling in Porphycene Seeded in a Supersonic Jet. *Chem. Phys. Lett.* **1998**, *296*, 549−556.
(59) Douhal, A.; Lahmani, F.; Zehnacker-Rentien, A.; Amat-Guerri, F. Excited-State Proton (or Hydrogen-Atom) Transfer in Jet-Cooled 2-(2′-Hydroxyphenyl)-5-Phenyloxazole. *J. Phys. Chem.* **1994**, *98*, 12198−12205.
(60) Sepiol, J.; Grabowska, A.; Borowicz, P.; Kijak, M.; Broquier, M.; Jouvet, C.; Dedonder-Lardeux, C.; Zehnacker-Rentien, A. Excited-State Intramolecular Proton Transfer Reaction Modulated by Low-Frequency Vibrations: An Effect of an Electron-Donating Substituent on the Dually Fluorescent Bis-Benzoxazole. *J. Chem. Phys.* **2011**, *135*, 034307.
(61) Muhlpfordt, A.; Bultmann, T.; Ernsting, N. P.; Dick, B. Excited-State Intramolecular Proton-Transfer in Jet-Cooled 3-Hydroxyflavone - Deuteration Studies, Vibronic Double-Resonance Experiments, and Semiempirical (Am1) Calculations of Potential-Energy Surfaces. *Chem. Phys.* **1994**, *181*, 447−460.
(62) Henchy, C.; Murray, C.; Crepin, C.; McCaffrey, J. G. A DFT Study of Reversed Isotope Shifts in H/D Substitution of Free-Base Porphyrin and Related Free-Base Tetrapyrroles. *Can. J. Chem.* **2012**, *90*, 1078−1091.
(63) Homayoon, Z.; Bowman, J. M.; Evangelista, F. A. Calculations of Mode-Specific Tunnelling of Double-Hydrogen Transfer in Porphycene Agree with Illuminate Experiment. *J. Phys. Chem. Lett.* **2014**, *5*, 2723−2727.